

Synthesis and Electrochemical Properties of LaFeO₃ Oxides Prepared Via Sol–Gel Method

Mahmoud Lebid · Mahmoud Omari

Received: 24 September 2011 / Accepted: 15 June 2012 / Published online: 16 November 2013
© King Fahd University of Petroleum and Minerals 2013

Abstract In this study, LaFeO₃ oxides were prepared by citric acid sol–gel method. The samples were subjected to various calcination temperatures in order to investigate the physicochemical properties of the oxide affected by the parameter. Samples were characterized by XRD, TG/DTA, IR, laser granulometry and cyclic voltammetry. By imposing various calcination temperatures, phase evolutions were observed. However, the calcination temperature affects significantly the particle size and catalytic activity of the oxide at higher temperature. Oxygen evolution shows that the current density at 1,050 °C is five times greater than at 950 °C. From these results, the best calcination temperature can be chosen to arrive at the effective catalyst necessary for the desired catalytic reaction.

Keywords Perovskite · LaFeO₃ · Powder diffraction · Thermal analysis · Electrochemical properties

الخلاصة

تم - في هذه الدراسة - إعداد أكاسيد LaFeO₃ بواسطة طريقة حامض الليمون محلول-تخثر. وتعرضت هذه العينات لدرجات حرارة تكليس مختلفة من أجل فحص الخصائص الفيزيائية للأكسيد الخاضع لهذا المتغير. وتم تمييز العينات باستخدام الأشعة السينية، وتحليل حراري، والأشعة تحت الحمراء، وحجم الحبيبات بالليزر والفولتامترية. وبعد استخدام درجات حرارة مختلفة لوحظت تطورات الحالة. ومع ذلك، درجة حرارة التكليس تؤثر تأثيراً كبيراً في حجم الجسيمات والنشاط التحفيزي. إن تطور الأوكسجين يظهر أن الكثافة الكهربائية عند 1050°C هي خمس مرات أكبر من 950°C. ومن هذه النتائج، فإنه يمكن اختيار أفضل درجة حرارة التكليس للوصول إلى حافز فعال للتفاعل التحفيزي المطلوب.

1 Introduction

Perovskite-type oxides have attracted great interest in both applied and fundamental areas of solid-state chemistry, physics, advanced materials and catalysis [1]. In particular, perovskites have been widely studied in recent years as deep oxidation catalysts due to their relatively low cost, high activity and thermal stability, which make them potential alternatives to noble metals in environmental power generation (NO_x and unburned hydrocarbons control) and exhaust clean-up (volatile organic compounds removal, automobile converters). Much attention has particularly been paid to lanthanum-transition metal-based perovskite oxides, which were introduced into catalysis some 30 years ago [2,3].

This work envisages the use of perovskite-type materials as anodes for extractive metallurgical processes. The LaFeO₃ is identified to thrive as a suitable electrode for O₂ evolution in alkaline system due to its high electronic conductivity and thermal stability. It is a *p*-type semiconductor catalytic material of perovskite structure (ABO₃). Its gas sensing properties, especially for toxic and noxious gases of NO₂ and CO are reported [4]. Although, there are many studies of preparation of LaFeO₃ oxides [4–8], few works have been carried out on the effect of the calcined temperature on the processes of formation of perovskite-like LaFeO₃ nanocrystals, structural and electrochemical properties of LaFeO₃ oxides.

In our present work, lanthanum ferrite has been synthesized by the citric acid sol–gel method using absolute alcohol as solvent and characterized for its physicochemical properties. The effect of the calcined temperature on the phase formation processes, particle size and electrochemical performance of this material is presented.

M. Lebid (✉) · M. Omari
Laboratory of Molecular Chemistry and Environment,
University of Biskra, B.P. 145, 07000 Biskra, Algeria
e-mail: m2omari@yahoo.fr

2 Experimental

Lanthanum ferrite was synthesized by the citric acid sol–gel method. Aqueous solutions of $\text{La}(\text{NO}_3)_2 \cdot 6\text{H}_2\text{O}$ (Biochem) and $\text{Fe}(\text{NO}_3)_3 \cdot 9\text{H}_2\text{O}$ (Biochem) were first dissolved in absolute ethanol separately. The molar amount of citric acid was equal to total molar amount of metal nitrates in solution. Citric acid (Biochem) was added to the precursors under vigorous stirring. The obtained solution was heated at 110°C for 12 h and calcined from 400 to $1,050^\circ\text{C}$ under air to obtain the final powder.

TGA and DTA analyses of the precursor were carried out using a Linseis STA PT1600 thermal analyzer with a heating rate of 10°C per minute and under atmospheric conditions. XRD characterization of samples was carried out with a D8 Advance-Brucker using a $\text{CuK}\alpha$ line at 0.1540 nm . IR spectra were recorded using FTIR-Shimadzu 8400S spectrometer. Powder size distribution was characterized with a laser particle size analyzer (Mastersizer 2000, Malvern).

The electrochemical experiments for O_2 reduction and evolution were performed using a Volta Lab 40 potentiostat/galvanostat. The measurements were carried out in a three-compartment cell. Potassium hydroxide electrolyte solution (1 M) was prepared by dissolving the required amount of KOH (Merck) into bidistilled water. The working electrodes (1 cm^2) were obtained by painting, with an oxide suspension. The loading of catalyst films was $12 \pm 3\text{ mg cm}^{-2}$ in each case. The counter electrode used was a Pt plate. The reference electrode was Hg/HgO/ 1 M KOH. All potentials in the text have been referred to this reference electrode.

3 Results and Discussions

3.1 TG/DTA Analysis

A typical TGA and DTA curves heating from 25 to 900°C for the LaFeO_3 precursor is shown in Fig. 1. The TGA curve exhibits five weight loss stages at the temperature ranges of 25 – 180 , 180 – 270 , 270 – 380 , 380 – 550 and 550 – 630°C . The DTA curve exhibits one broad endothermic peak at 120°C , three strong exothermic peaks at about 180 , 350 and 510°C and two weak exothermic peaks at about 230 and 620°C .

The first gradual weight loss step from 25 to 180°C accompanying with a broad endothermic peak and a strong exothermic peak can be ascribed to the removal of the residual water and a partial decomposition of citric acid chain. The second weight loss stage at the temperature range of 180 – 270°C accompanying with a weak exothermic peak corresponds to the decomposition of citrates and some of the nitrates. The third small weight loss from 270 to 380°C associating with the strong exothermic peak at about 350°C

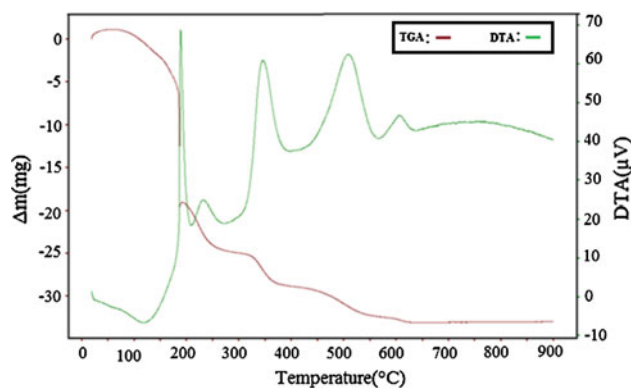


Fig. 1 TG and DTA curves of LaFeO_3 precursor heated in air at $10^\circ\text{C min}^{-1}$

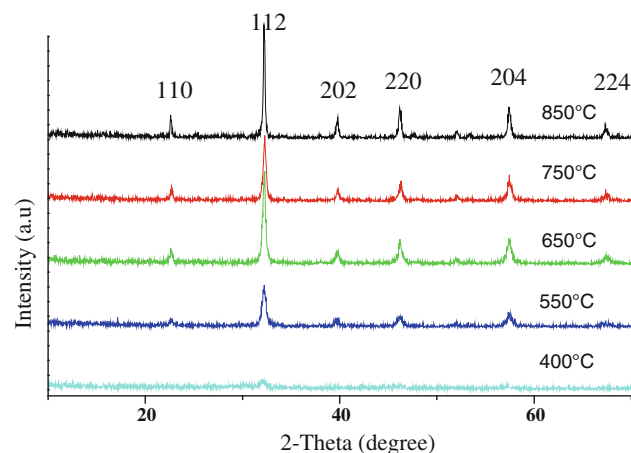


Fig. 2 XRD patterns of the powders LaFeO_3 calcined at different temperatures

corresponds probably to the remaining organic matter and formation of the disordered La_2O_3 [9]. The fourth weight loss from 380 to 550°C accompanying with a strong exothermic peak corresponds to the combustion of residual carbon and nitrates. A weak weight loss above 550°C was detected. It was accompanied with a small exothermic peak which can be attributed to the formation of the LaFeO_3 crystal. There is no weight loss above 630°C .

3.2 X-ray Diffraction

Figure 2 presents XRD patterns of LaFeO_3 calcined at different temperatures. After being heated at 400°C in air, the powder is almost amorphous. When the powder is calcined at $T \geq 550^\circ\text{C}$, the amorphous phase disappears and the characteristic peaks of the perovskite phase appear with low intensity, which signified the transformation of amorphous phase to the crystalline pure orthorhombic phase. The crystallinity of the LaFeO_3 phase is improved with increasing calcination temperature. Further heating only increased the intensity of the X-ray peaks, and no other phase peaks are observed.

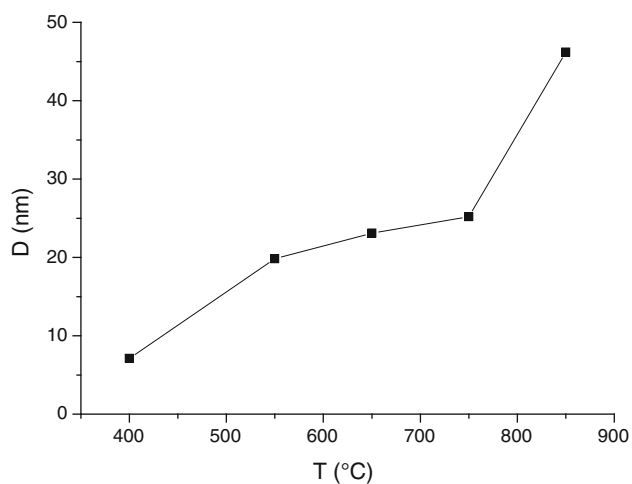


Fig. 3 Crystallite size of LaFeO₃ samples calcined at different temperatures

The same result was also reported using a bio-inspired method [10] and another based on the thermal decomposition of a cyanide-bridged heteronuclear complex, La[Fe(CN)₆]·5H₂O [5], indicating that LaFeO₃ begins to crystallize into the pure orthorhombic structure at 600 °C and its crystallinity increases with increasing calcination temperature.

While using the co-precipitation method [5], XRD patterns at different temperatures indicate that the perovskite phase becomes pure at the calcining temperature above 800 °C. The peak broadening at lower angle is more meaningful for the calculation of particle size, therefore, size of nanocrystals has been calculated using Debye–Scherrer formula [11]. This formula for crystallite size determination is given by:

$$D = 0.89\lambda / \beta \cos\theta \quad (1)$$

where D is the crystallite size, λ is the wavelength of X-ray, β is the full width at half maximum (β expressed in radians), θ is the Bragg's angle. The particle size obtained from XRD for different calcination temperatures is presented in Fig. 3. From this figure, it is clear that the crystallite size increases with increasing temperature and it is substantial after heating to above 750 °C. It was attributed to a typical effect of temperature on crystal growth. The same trend was also found for LaFeO₃ prepared by a sol–gel method using glycine as a chelating agent [12].

3.3 IR Spectroscopy

The FTIR spectra of LaFeO₃ precursor and calcined powder at different temperatures recorded in the range 400–4,000 cm⁻¹ are shown in Fig. 4. The broad absorption band at 3,440 cm⁻¹ is associated with the O–H stretch of intermolecular hydrogen bonds or molecular water. The sharp absorp-

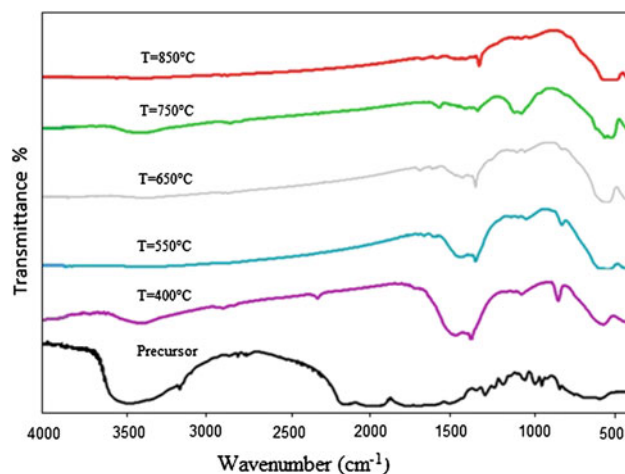


Fig. 4 Infrared spectra of powder LaFeO₃ calcined at different temperatures

tion band at 1,120 cm⁻¹ can be attributed to the vibrational mode of carbonates. The band at 855 cm⁻¹ corresponds to nitrate ions.

After calcining the LaFeO₃ precursor for 6 h, the bands corresponding to carbonates and nitrates disappear and two new bands at 560 and 450 cm⁻¹ are observed. These bands are assigned to Fe–O stretching vibration and O–Fe–O deformation vibration, respectively [13]. It can be observed that most organic species in the precursor powders disappeared after calcination between 550 and 650 °C which coincides with the XRD analysis discussed earlier. It is observed that the band positions are the temperature-dependent.

The bands displacement is so light that it is only noticed when comparing spectra of calcined compounds at 400 and 850 °C. This may be due to the slight effect of temperature on the distribution of ions in the structure.

3.4 Particle Size Analysis

Figure 5 presents the particle distribution of LaFeO₃ calcining at different temperatures. After heating, the ceramics are made of small grains of diameter smaller than 0.8 μm. However, these grains agglomerate. This is clearly revealed by laser granulometry, as shown in Fig. 5, which presents the percentage of volume occupied by the grains for a particular diameter.

The powder has been ultrasonically treated in situ in water for 15 min. The presence of two or three well-defined peaks for all temperatures show that most of the grains are aggregated. The grain size is centered around 1.2–18.69 μm and the aggregate sizes are around 14–55 μm. The grain size is observed to increase with the calcination temperature increasing. This trend shows well the crystallite size-temperature dependency. Dai et al. [12] reported also that the crystalline size of LaFeO₃ oxide prepared using the

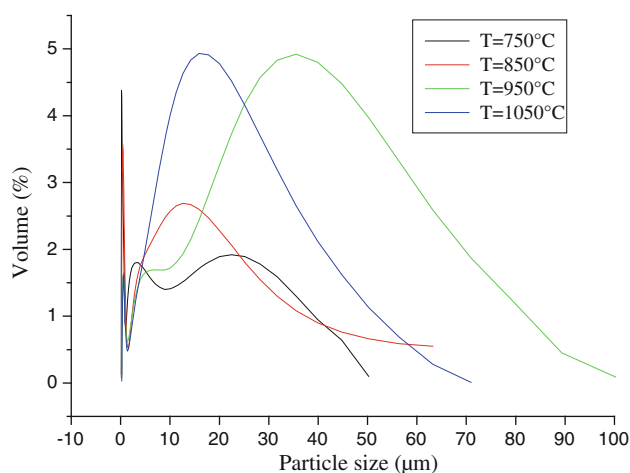


Fig. 5 Particle size distribution of LaFeO₃ samples calcined at different temperatures

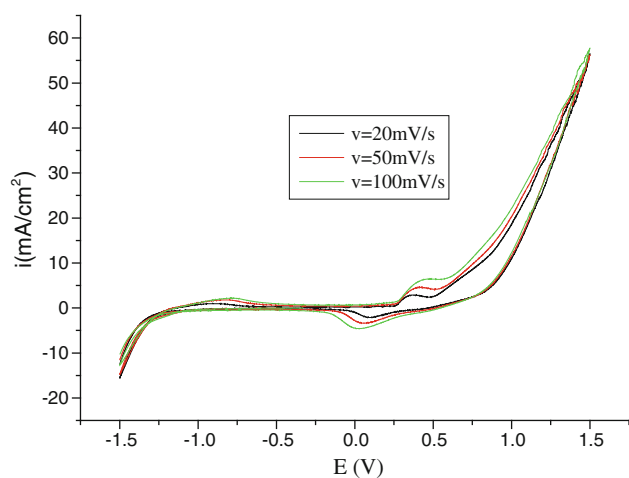


Fig. 6 Cyclic voltammograms of LaFeO₃ calcined at 950 °C. Scan rates: from 20 to 100 mV s⁻¹

same synthesis method increases from 31.7 to 53.5 nm with increasing calcination temperature in the range 800–1,000 °C, while the specific surface area decreases from 12.56 to 2.36 m² g⁻¹. The crystallite size results exhibit the same trend with increasing calcination temperature (Fig. 3).

Similar results were found with LaCoO₃ oxide [14]. Indeed, the grain size and the crystal size of LaCoO₃ increased with the calcination temperature from 500 to 800 °C using an amorphous complex as a precursor. This indicates that the calcination temperature has a serious effect on the grain size and the crystallite size of these oxides.

3.5 Electrochemical Properties

Electrochemical Behavior of LaFeO₃ Electrodes

Figure 6 presents the voltammogram of LaFeO₃ oxide at three scan rates calcined at 950 °C. We find in general that this

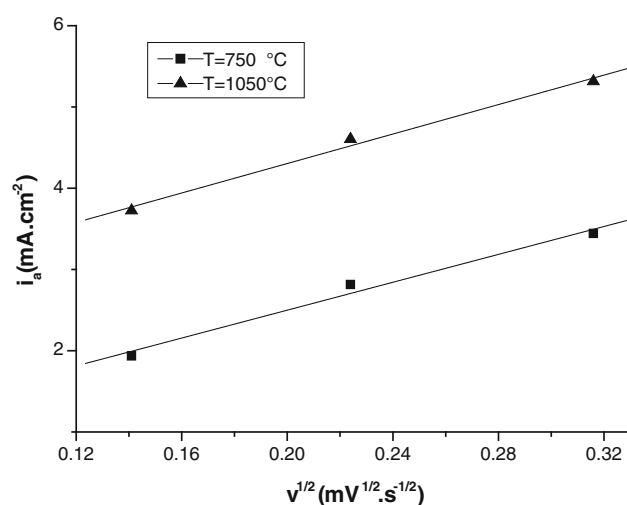


Fig. 7 Anodic current density of LaFeO₃ as a function of a square root of the scan rate

electrode has a qualitatively similar behavior. The voltammograms at scan rate of 20, 50 and 100 mV s⁻¹ exhibit two redox peaks, an anodic ($E_{pa} = 379, 417$ and 490 mV) and a corresponding cathodic ($E_{pc} = 102, 59$ and 26 mV) peak, respectively, prior to the onset of the O₂ evolution reaction, revealing a pseudo-capacitance due to the Ni(III)/Ni(II) surface redox couple [15].

Indeed there is, in all cases before the release of oxygen, the appearance of an oxidation peak. During the scan back, a reduction peak is observed at lower potential. These peaks are probably due to the couple Ni(II)/Ni(III) from the nickel substrate [16] according to the reaction:



This result means that in anodic branch OH⁻ ions are electro-adsorbed in the Ni(III) active sites of the oxide surface prior to oxygen evolution. An increase in scan rate shifted the anodic peak to more positive, probably due the effect of ohmic resistance of the oxide.

With the increasing scan rate both anodic and cathodic current increases and the cathodic peak potentials have shifted towards negative values, while anodic peak potentials move to more positive values. This observation suggests that the electrode process is diffusion controlled. Anodic peak currents corrected for capacitive currents to the electrodes calcined at two temperatures vary linearly with the square root of the scan rate (Fig. 7). This linear relation appears also in favor of the fact that the redox reaction is controlled by a process of diffusion of ions in the material.

Electro-Catalytic Activity of LaFeO₃ Oxides

The electrochemical activity for oxygen reduction and evolution reactions was investigated on LaFeO₃-coated nickel sub-

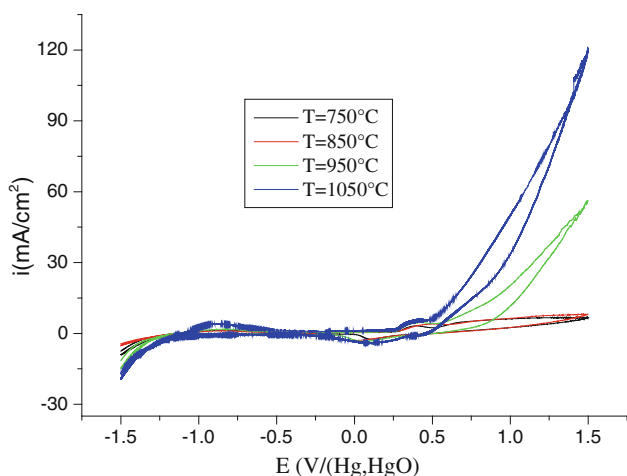


Fig. 8 The i - E polarization curves of oxygen evolution and reduction for LaFeO_3 electrodes calcined at different temperatures in 1 M KOH

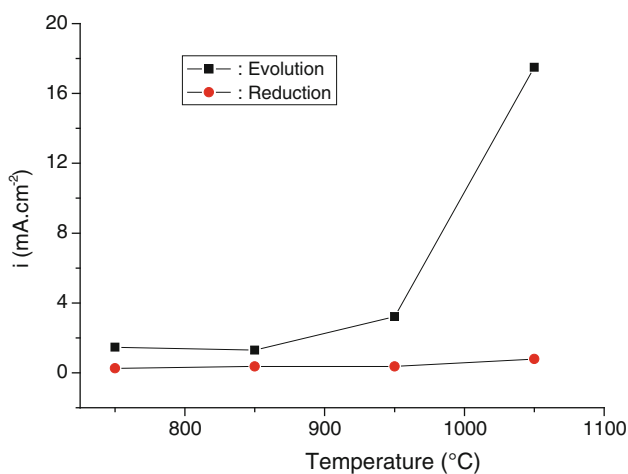


Fig. 9 Electrode performance as a function of temperature at $E = -1$ and 0.8 V for oxygen reduction and evolution for LaFeO_3

strate. Polarization studies under potentiostatic conditions were carried out. Figure 8 shows the anodic and cathodic current-potential curve of air electrode at different temperatures. The coated electrode films showed good adherence during polarization. The voltammetric profile is rather featureless, showing a wide plateau region. It is clear that the coated perovskite electrodes present a wide range of electrochemical stability and a temperature dependency of the current intensity.

Electrode reactions over the surface of the oxides exhibit high currents. Calcined compounds at high temperature show higher anodic or cathodic currents than those at lower one. Compared to all samples, the LF_{1050} (LaFeO_3 calcined at $1,050$ °C) one appears to be more active. As the temperature increases the catalytic activity will also increase and provides a catalyst with high crystallite size. Figure 9 presents the anodic and cathodic current densities obtained at potentials of $E = -1$ and 0.8 V, respectively.

The highest electrode performance is achieved, for both cases, with the sample calcined at higher temperature. Oxygen evolution reaction shows an important jump for $T > 950$ °C where the current density at $1,050$ °C ($i_a = 17.5$ mA cm^{-2}) is five times greater than at 950 °C ($i_a = 3.22$ mA cm^{-2}), while in the oxygen reduction reaction, the response of the oxide is less visible and the maximum current density produced at $1,050$ °C is 0.79 mA cm^{-2} . This result is in good agreement with those reported by Einaga et al. [17] on the benzene oxidation over LaMO_3 ($M = \text{Mn, Co and Fe}$) perovskite catalysts.

The catalytic performance of the LaFeO_3 sample is relevant with the crystalline size and the rate of oxygen migration from bulk toward surface [12]. In fact, Dai et al. reported that as the calcination temperature increases in the range 800 – $1,100$ °C, the crystalline size increases. This trend agrees well with the average particle size determined from the XRD pattern parameters of the LaFeO_3 oxide (Fig. 3).

These results show clearly that the catalytic behavior of iron oxide samples is consistent with their particles size where smaller particles size was obtained at higher calcination temperature. Indeed, the particle size dependence of catalyst performance is consistent with the fact that the surface structure and electronic properties change greatly with the particle size.

Recent works reported that surface area of LaFeO_3 at different temperatures decreases with increasing temperature [12,17]. This indicates clearly that the surface area of this compound as the determining factor in the reduction and evolution rates should be excluded, as the electrochemical activity electrode does not increase with its surface area.

Berenov et al. [18] reported an increase in the measured values of the conductivity with increasing the calcination temperature for LaFeO_3 oxide. Indeed, conductivity values obtained at 750 , 850 , 950 and $1,050$ °C are 0.13 , 0.15 , 0.20 and 0.31 S cm^{-1} , respectively. This was probably due to the increase of oxygen vacancies generated with increasing temperature. This is in good agreement with measured Seebeck coefficients of LaFeO_3 which upon heating indicates the increase in the positive values that can be ascribed to the increase in the concentration of positively charged oxygen vacancies generated intrinsically [19]. The temperature dependence of oxygen vacancies in LaFeO_3 oxide was also reported by Levasseur and Kaliaguine [20]. In fact, TPD- O_2 experiments show two types of desorbed oxygen species: the one coming from the surface (α -oxygen) at $T < 750$ °C and the other from the bulk (β -oxygen) at $T > 750$ °C, thus leading to the creation of anionic vacancies.

Consequently, from these results it is suggested that oxygen ion transport plays a predominant role in the overall electrical conduction in LaFeO_3 . This correlation between the activity and the conductivity evinces the key role of the

electrical parameter as a determining factor in the reaction kinetics.

4 Conclusion

This study establishes the effect of calcination temperature on the physicochemical properties of the lanthanum ferrite, prepared by citric acid sol–gel method. Phase evolution was clearly seen as the temperature was varied. However, the various calcination temperatures were found to make a significant impact on the particle size and their distribution of the samples at higher temperature. This was fully supported by particle size measurements. In electrochemical study, LF₁₀₅₀ electrode exhibits significantly greater electroactivity, indicating that this material is the best electrocatalyst for oxygen reduction and evolution reactions in the investigated temperature range. These results indicate clearly the correlation between the electrical conductivity and the electrochemical activity in these compounds.

References

- Tejuca, J.L.; Fierro, J.L.G.: Properties and Applications of Perovskite-Type Oxides. Marcel Dekker, New York (1993)
- Saracco, G.; Cerri, I.; Specchia, V.; Accornero, R.: Catalytic pre-mixed fibre burners. Chem. Eng. Sci. **54**, 3599 (1998)
- Poplawski, K.; Lichtenberger, J.; Keil, F.J.; Schnitzlein, K.; Amiridis, M.D.: Catalytic oxidation of 1,2-dichlorobenzene over ABO₃-type perovskites. Catal. Today **62**, 329 (2000)
- Bai, S.; Shi, B.; Ma, L.; Yang, P.; Liu, Z.Y.; Li, D.Q.; Chen, A.F.: Synthesis of LaFeO₃ catalytic materials and their sensing properties. Sci. China Ser. B **52**, 2106 (2009)
- Nakayama, S.: LaFeO₃ perovskite-type oxide prepared by oxide-mixing, co-precipitation and complex synthesis methods. J. Mater. Sci. **36**, 5643 (2001)
- Tien, N.A.; Mittova, I.Ya.; Almjasheva, O.V.; Kirillova, S.A.; Gusarov, V.V.: Influence of the preparation conditions on the size and morphology of nanocrystalline lanthanum orthoferrite. Glass Phys. Chem. **34**, 756 (2008)
- Popa, M.; Frantti, J.; Kakihana, M.: Lanthanum ferrite LaFeO_{3+d} nanopowders obtained by the polymerizable complex method. Solid State Ion. **154–155**, 437 (2002)
- Chandradass, J.; Kim, K.H.: Nano-LaFeO₃ powder preparation by calcining an emulsion. Mater. Chem. Phys. **122**, 329 (2010)
- Sadaoka, Y.; Aono, H.; Traversa, E.; Sakamoto, M.: Thermal evolution of nanosized LaFeO₃ powders from a heteronuclear complex. La[Fe(CN)₆]*n*H₂O. J. Alloy. Compd. **278**, 135 (1998)
- Song, P.; Wang, Q.; Zhang, Z.; Yang, Z.: Synthesis and gas sensing properties of biomorphic LaFeO₃ hollow fibers templated from cotton. Sens. Actuators B-Chem. **147**, 248 (2010)
- Cullity, B.D.: Elements of X-ray Diffractions. Addison Wesley, Reading (1978)
- Dai, X.; Yu, C.; Li, R.; Wu, Q.; Shi, K.; Hao, Z.: Effect of calcination temperature and reaction conditions on methane partial oxidation using lanthanum-based perovskite as oxygen donor. J. Rare Earth. **26**, 341 (2008)
- Shivakumara, C.: Low temperature synthesis and characterization of rare earth orthoferrites LnFeO₃ (Ln = La, Pr and Nd) from molten NaOH flux. Solid State Commun. **139**, 165 (2006)
- Zhu, Y.; Tan, R.; Yi, T.; Ji, S.; Ye, X.; Cao, L.: Preparation of nanosized LaCoO₃ perovskite oxide using amorphous heteronuclear complex as a precursor at low temperature. J. Mater. Sci. **35**, 5415 (2000)
- Abdel Rahim, M.A.; Abdel Hameed, R.M.; Khalil, M.W.: Nickel as a catalyst for the electro-oxidation of methanol in alkaline medium. J. Power Sources **134**, 160 (2004)
- Tiwari, S.K.; Chartier, P.; Singh, R.N.: Preparation of perovskite-type oxides of cobalt by malic acid aided process and their electrocatalytic surface properties in relation to oxygen evolution. J. Electrochem. Soc. **142**, 148 (1995)
- Einaga, H.; Hyodo, S.; Teraoka, Y.: Complete oxidation of benzene over perovskite-type oxide catalysts. Top. Catal. **53** 629 (2010)
- Berenov, A.; Angeles, E.; Rossiny, J.; Raj, E.; Kilner, J.; Atkinson, A.: Structure and transport in rare-earth ferrates, Solid State Ion. **179**, 1090 (2008)
- Iwasaki, K.; Ito, T.; Yoshino, M.; Matsui, T.; Nagasaki, T.; Arita, Y.: Power factor of La_{1-x}Sr_xFeO₃ and LaFe_{1-y}Ni_yO₃. J. Alloy. Compd. **430**, 297 (2007)
- Levasseur, B.; Kaliaguine, S.: Methanol oxidation on LaBO₃ (B = Co, Mn, Fe) perovskite-type catalysts prepared by reactive grinding. Appl. Catal. A-Gen. **343**, 29 (2008)

